GeoScienceWorld
Lithosphere
Volume 2022, Article ID 6780739, 15 pages
https://doi.org/10.2113/2022/6780739

Lithosphere

Research Article

Investigation on Mechanism of Coal Burst Induced by the Geological Weak Surface Slip in Coal Seam Bifurcation Area: A Case Study in Zhaolou Coal Mine, China

Zong-long Mu,[1] **Jing Yang**,[2] **Guang-jian Liu**,[3] **Yu-chen Zhang**,[1] **and Jian-hang Jiao**[1]

[1]*Jiangsu Engineering Laboratory of Mine Earthquake Monitoring and Prevention, School of Mines, China University of Mining and Technology, Xuzhou 221116, China*
[2]*State Key Laboratory for Geomechanics and Deep Underground Engineering, School of Mechanics and Civil Engineering, China University of Mining and Technology, Xuzhou 221116, China*
[3]*Key Laboratory of Rock Mechanics and Geohazards of Zhejiang Province, Shaoxing University, Shaoxing, Zhejiang 312099, China*

Correspondence should be addressed to Jing Yang; yj986628415@163.com

Received 9 May 2022; Accepted 20 June 2022; Published 8 July 2022

Academic Editor: Wenzhuo Cao

The coal seam bifurcation area (CSBA) exists widely in coal measure strata, where the geological weak surface (GWS) slip in overburden structure is easy to induce coal burst. The coal mass of coal face shows overall instability failure and high-speed throwing characteristics during the coal burst, seriously threatening the safe and efficient coal mine production. In order to understand the GWS-induced coal burst caused by the slip in CSBA and find the main controlling factors of GWS slip, the GWS slip criterion in CSBA was established based on the coal burst case analysis of overburden structure in CSBA of 1305 coal face (1305CF) in Zhaolou Coal Mine. The case study showed that the angle and range of CSBA are the main controlling factors affecting GWS slip. The FLAC3D numerical model of CSBA was established to analyze the influence effect of main control factors. The results show that the increase of angle and range of CSBA will increase the influence scope and degree of coal face mining, improving coal face burst risk. However, the peak point region of abutment pressure will not be affected, gradually reaching its peak within 0 m ~10 m from the coal seam merging area. With the increase of the angle of CSBA, the integrity of the triangular wedged rock mass along the GWS slip will be enhanced, aggravating the dynamic disturbance to the coal mass. With the increase of the range of CSBA, the slip of triangular wedged rock mass along GWS gradually changes from integral slip to phased slip, which will intermittently disturb the coal mass of the coal face. The research results have certain theoretical significance and practical value for preventing and controlling coal bursts in CSBA.

1. Introduction

As a typical dynamic disaster, coal burst is usually accompanied by the sudden and sharp throwing of coal-rock mass, destroying the roadway support system and mining equipment and resulting in casualties and economic losses [1–5]. Many researchers have made fruitful research achievements on monitoring, early warning, and disaster prevention of coal bursts in different engineering cases in recent decades. Monitoring and early warning technologies [6–10] such as microseismic monitoring, seismic computed tomography, bursting strain energy index monitoring, drilling cuttings method, and spatiotemporal monitoring of mine seismic activity have formed. In addition, prevention and control technologies [11–14], including pressure relief with large diameter drilling of coal mass, softening of coal seam by water injection, and hard roof pre splitting blasting, have been developed. It is generally believed that the coal burst mechanism is that coal-rock mass accumulates a large amount of elastic energy under high ground stress (static load), and the excessive elastic energy is suddenly released in the form of kinetic energy under the dynamic disturbance (dynamic load) around the stope, resulting in large-scale strength instability of coal-rock mass. It is also known as

the dynamic and static load superposition induce coal burst principle [15–18].

Burst monitoring and prevention measures can be implemented in the project site based on the principle of dynamic and static load superposition-induced coal burst by analyzing the mechanical characteristics of coal-rock mass, the source of dynamic and static loads, and the main body of energy release when coal burst occurs, to minimize the occurrence probability and failure intensity of dynamic disasters. However, fault, fold, GWS, and other geological structures are widely distributed in the stratum due to the complexity of underground engineering geological conditions. In addition, the surrounding rock of the project site is usually under the complex stress conditions of "three high and one disturbance" (high ground stress, high ground temperature, high osmotic pressure, and mining disturbance), making it difficult to prevent coal burst. Coal burst can be divided into four types: coal pillar compression type [19, 20], folding structure type [21], roof breaking type [4, 22], and fault slip type [23, 24]. These coal bursts are induced by the superposition of dynamic and static loads caused by mining technical factors and geological structure factors. However, there is a special structure in coal measure strata, called CSBA, which the GWS usually represents at the CSBA. According to the sedimentological theory and the analysis method of basin evolution, the erosion of the distributary channel to the lower coal seam and the differential compaction of sediment accumulation in the process of coal formation causes a large area of coal seam thinning zone and CSBA of Shanxi Formation No. 3 coal seam in Southwest Shandong [25].

In recent years, many coal burst accidents have occurred in the CSBA. The coal face presents overall instability failure and high-speed throwing characteristic during the coal burst, which is a new type. Figure 1 shows a schematic diagram of the coal burst accident in the CSBA of 1305CF in Zhaolou Coal Mine in Shandong Province. A serious coal burst accident occurred when the coal face was mined in this area on July 29, 2015. It was demonstrated that the slip of GWS in the CSBA was the main cause of the accident [26]. Many researchers have studied many typical coal burst cases, especially the fault slip induced coal burst mechanism and monitoring and prevention in large-scale GWS [23, 27–29], while there are few studies on the slip induced coal burst mechanism of GWS in medium-scale CSBA. The incubation mechanism of coal burst in the CSBA is still unclear during mining.

In this study, GWS slip criterion in CSBA will be established based on the coal burst accident case of 1305CF in Zhaolou Coal Mine by considering the mechanical characteristics of GWS in CSBA under two states of original rock stress and mining disturbance. Further analysis reveals the main controlling factors affecting GWS slip. Based on FLAC3D numerical simulation, the stress evolution of surrounding rock and the mechanical response characteristics of GWS in CSBA under different influencing factors will be analyzed to understand the mechanism of coal burst induced by GWS slip in CSBA. The findings have important theoretical significance and application value for the prevention and control of coal burst in the CSBA.

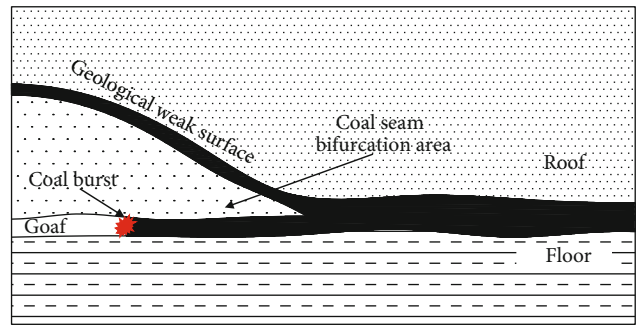

Figure 1: Schematic diagram of coal burst accident in CSBA of 1305CF.

2. Situation of Coal Burst Accident Case in CSBA

2.1. Geological Situation of 1305CF. 1305CF is located in the No. 1 mining district of Zhaolou Coal Mine (see Figure 2), adjacent to the track dip roadway of No. 1 mining district in the east and the boundary of No. 7 mining district in the west, affected by the F14 fault. The 1304CF, 1306CF, and 1307CF, around 1305CF, have all been mined. Therefore, the 1305CF is an isolated coal face with special surrounding rock structures such as goafs on both sides and adjacent to faults on one side. The main coal seam of the coal face is 3# coal seam and 3# lower bifurcation coal seam, with a strike length of 618.41 m, dip length of 136.52 m, and burial depth of about 950 m. The dip angle of the coal seam is 0 ~ 11°, with a mean of 4.7°. The coal seam thickness is 1.0 m ~ 8.4 m, with a mean of 5.1 m.

Figure 3 shows the comprehensive column illustration of coal and rock strata in the 1305CF. The immediate roof of the coal face mainly consists of mudstone and sandy mudstone, and the main roof with an average thickness of 10.18 m is fine sandstone. The thickness of the upper layer in the 3# coal seam in the CSBA is 1.0 m ~ 1.7 m, with an average of 1.13 m, while the thickness of the lower layer is 2.7 m ~ 6.4 m, with an average of 4.25 m. The dirt band in the CSBA is mainly sandy mudstone. The bifurcation interval is 0.7 m ~ 14.6 m, with an average of 7.59 m. According to the laboratory test of China University of Mining and Technology, No. 3 coal seam, roof, and floor have a strong bursting tendency.

2.2. Analysis on Inducement of Coal Burst Accident in CSBA. A coal burst accident occurred at 1305CF on July 29, 2015 [26]. The coal face was in the stage of trial mining when the accident occurred. As shown in Figure 4, mining area A is the underlayer of 3# coal seam. According to the situation of coal thrown out on site, the center point of the coal burst is located in the No. 53-No. 64 hydraulic support section. The accident caused serious damage to the coal face and two roadway areas. The location of the coal burst is shown in Figure 4. The situation of destruction on site is shown in Figure 5.

It is known from the accident identification that the coal burst accident happens in the mining stage from the lower

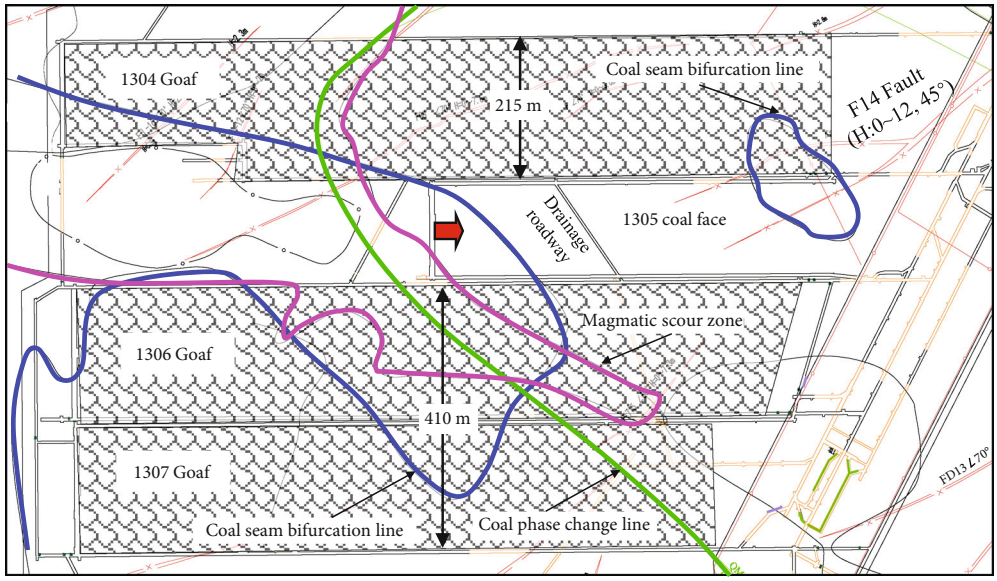

Figure 2: Geological and mining situation around 1305CF.

Lithology name	Geological formations	Level (m)	Thickness (m)
Coarse mudstone		−893.95	4.15
Sandy mudstone		−898.10	12.28
Fine sandstone		−910.38	8.74
Mudstone		−919.12	2.86
Fine sandstone		−921.80	10.18
Mudstone		−931.98	6.78
3 upper coal		−938.76	1.13
Sandy mudstone		−946.35	7.59
3 lower coal		−950.60	4.25
Siltstone		−957.11	6.51
Mudstone		−965.74	8.63
Medium sandstone		−972.67	6.93

Figure 3: Geological formations in the 1305CF.

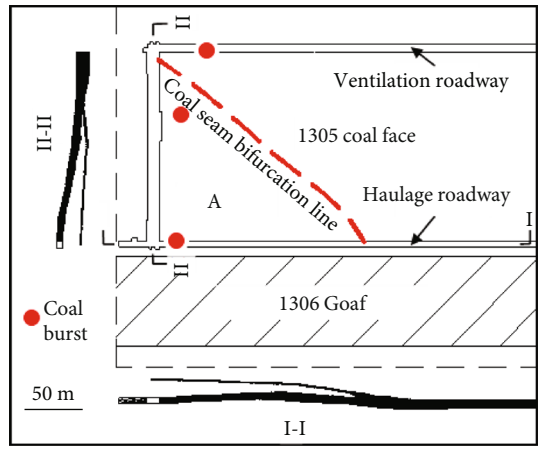

Figure 4: Coal burst locations in 1305CF.

layer of the CSBA to the coalbed merging area. In the mining process, the primary rock stress in the lower layer area is higher due to the influence of the buried depth and geological structure. The upper layer, which can be regarded as the GWS in the overburden of 1305CF, of the 3# coal seam is thin. The overall thickness of the dirt band regarded as an immediate roof is large. As shown in Figure 6, when the mining activity is close to the CSBA, the overlying strata and coal mass of the 1305CF will squeeze a triangular wedged dirt band, resulting in the activation of GWS. The triangular wedged dirt band slips upward relative to the overlying strata, and the uncollapsed dirt band at the rear of the coal face twists downward to squeeze the lower stratified coal mass, forming a clamping effect on the coal mass in front of the coal face between the dirt band and the floor of the 3# coal seam. As a result, the coal burst of coal mass of 1305CF occurred under the effect of high-stress clamping. The accident is a new type of coal burst and belongs to the coal burst type of coal mass overall instability in the coal face [25].

3. Slip Criterion of GWS in CSBA

Based on the accident analysis in Section 2.2, the main reason for this coal burst accident is the activation of the GWS formed by the upper stratification coal seam in the

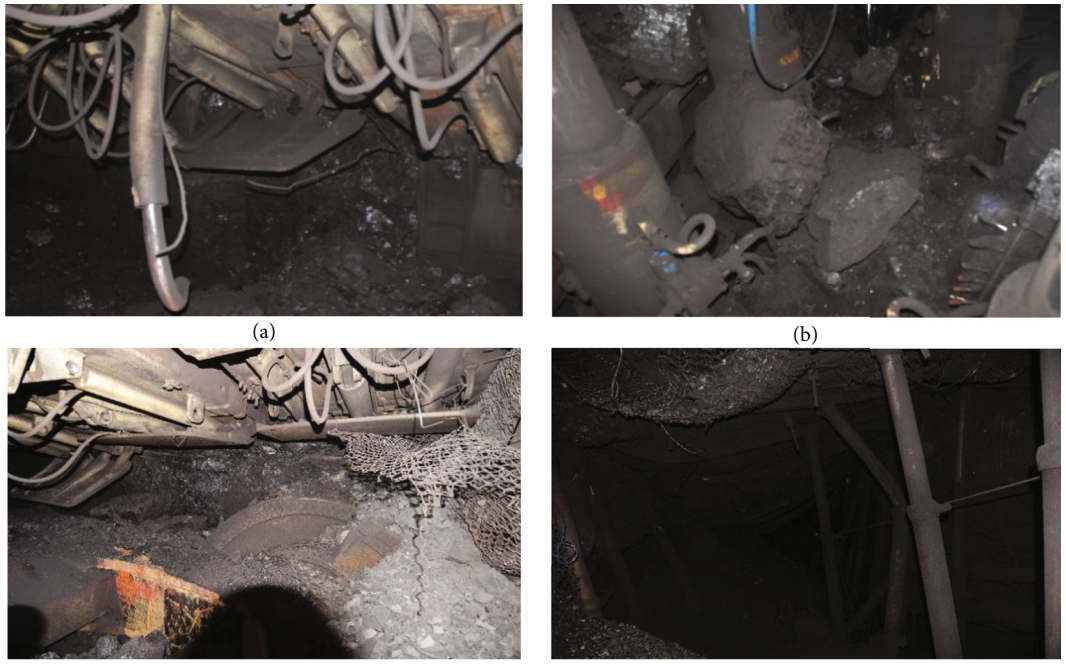

Figure 5: The situation of destruction in 1305CF. (a) Hydraulic support damaged. (b) Coal mass throwing. (c) Coal mining machine damaged. (d) Roadway deformation.

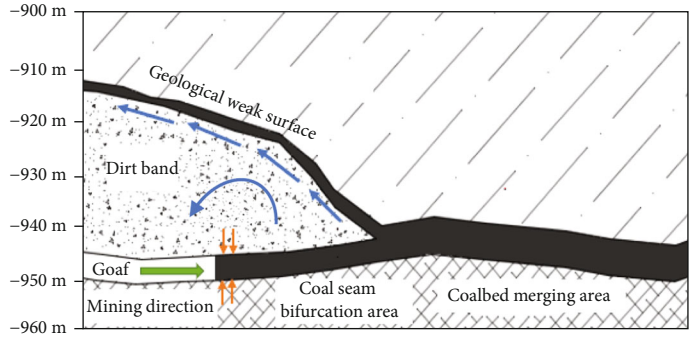

Figure 6: Schematic diagram of coal burst induced by dirt band shear slip in CSBA of 1305CF.

CSBA and the shear slip leading to compressive stress exceeding the ultimate strength of coal mass under dynamic and static load superposition. Therefore, the slip criterion of GWS in CSBA may be established to reveal the mechanism of coal burst induced by this type. Based on the overburden structure of CSBA in 1305CF, the roof of the CSBA can be simplified as a clamped beam under the original rock stress and simplified as a cantilever beam under the mining disturbance.

3.1. Under Original Rock Stress State. The stress diagram of CSBA under original rock stress is shown in Figure 7. R is the internal force at both ends of the rock beam, q is the uniformly distributed load strength above rock strata, and s is the strike length of the rock stratum. Point A with normal stress σ_x and tangential stress τ_x is the point on the GWS in CSBA.

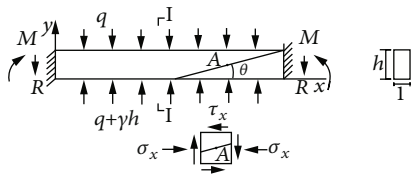

Figure 7: Stress analysis of any point on CSBA under original rock stress.

Assuming that the width of the beam is 1, the normal and tangential stresses are as follows:

$$\begin{cases} \sigma_x = \dfrac{12M(x)(y - h/2)}{h^3}, \\ \tau_x = \dfrac{3}{2}Q(x)\left(\dfrac{h^2 - 4y^2}{h^3}\right), \end{cases} \tag{1}$$

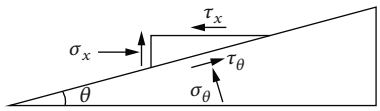

Figure 8: Stress analysis of any microelement at the coal-rock interface.

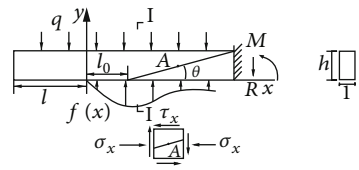

Figure 9: Stress analysis of any point on CSBA under mining disturbance.

where $M(x)$ is the bending moment of the section where the point is located, $Q(x)$ is the shear force of the section where the point is located, and y is the distance between the point and the neutral axis of the section. According to the equilibrium equation of the force, $M(x)$ and $Q(x)$ can be expressed as follows:

$$\begin{cases} M(x) = \dfrac{\gamma h s^2}{12} + \dfrac{\gamma h x^2}{2} - \dfrac{\gamma h s x}{2}, \\ Q(x) = \dfrac{\gamma h s}{2} - \gamma h x, \end{cases} \tag{2}$$

where γ is the rock bulk density, and h is the rock stratum thickness.

By substituting Eq. (2) into Eq. (1), the normal stress and tangential stress of any point A on the GWA of the CSBA can be obtained:

$$\begin{cases} \sigma_x = \dfrac{\left(\gamma h s^2 + 6\gamma h x^2 - 6\gamma h s x\right)(y - h/2)}{h^2}, \\ \tau_x = \left(\dfrac{3}{4}\gamma s - \dfrac{3}{2}\gamma x\right)\left(\dfrac{h^2 - 4y^2}{h^2}\right). \end{cases} \tag{3}$$

A section is made along the GWS of the CSBA, and a triangular microelement with a unit thickness is taken at the coal-rock interface. The stress analysis is shown in Figure 8.

According to the mechanical equilibrium equation of microelement, it can be obtained:

$$\begin{cases} \sigma_\theta \tan\theta + \tau_x = \sigma_x \tan\theta + \tau_\theta, \\ \tau_\theta \tan\theta + \tau_x \tan\theta = 0, \end{cases} \tag{4}$$

where θ is the angle of CSBA, σ_θ is the normal stress on GWS, and τ_θ is the tangential stress on GWS. Equation Eq. (4) can be further deduced as

$$\begin{cases} \sigma_\theta = \sigma_x \sin^2\theta - \tau_x \sin 2\theta, \\ \tau_\theta = \tau_x \cos 2\theta - \dfrac{1}{2}\sigma_x \sin 2\theta. \end{cases} \tag{5}$$

By substituting Eq. (3) into Eq. (5), the tangential stress and normal stress of GWS in CSBA under the original rock stress can be obtained.

$$\begin{cases} \sigma_\theta = \dfrac{\left(\gamma h s^2 + 6\gamma h x^2 - 6\gamma h s x\right)(y - h/2)}{h^2} \sin^2\theta - \left(\dfrac{3}{4}\gamma s - \dfrac{3}{2}\gamma x\right)\left(\dfrac{h^2 - 4y^2}{h^2}\right) \sin 2\theta, \\ \tau_\theta = \left(\dfrac{3}{4}\gamma s - \dfrac{3}{2}\gamma x\right)\left(\dfrac{h^2 - 4y^2}{h^2}\right) \cos 2\theta - \dfrac{\left(\gamma h s^2 + 6\gamma h x^2 - 6\gamma h s x\right)(y - h/2)}{2h^2}\sigma_x \sin 2\theta, \\ s - \dfrac{h}{\tan\theta} \le x \le s, 0 \le y \le \dfrac{h}{2}. \end{cases} \tag{6}$$

3.2. Under Mining Disturbance. The abutment pressure will appear in front of the coal face under the mining disturbance compared to the original rock stress, and the rock stratum needs to be simplified as a cantilever beam (see Figure 9).

Based on the force balance of the cantilever beam, it can be obtained.

$$\begin{cases} q\left(l + l_0 + \dfrac{h}{\tan\theta}\right) + R = \displaystyle\int_0^{l_0 + (h/\tan\theta)} f(x)dx, \\ M + \dfrac{q}{2}\left(l + l_0 + \dfrac{h}{\tan\theta}\right)^2 = \displaystyle\int_0^{l_0 + (h/\tan\theta)} f\left(l_0 + \dfrac{h}{\tan\theta} - x\right)dx, \end{cases} \tag{7}$$

$$\begin{cases} M(x) = \int_0^x f(x)xdx - \dfrac{q}{2}(l+x)^2, \\ Q(x) = q(l+x) - \int_0^x f(x)dx, \end{cases} \tag{8}$$

where l is the suspended length of the immediate roof, l_0 is the distance from the coal face to the coal seam bifurcation point, and $f(x)$ is the front abutment stress of the coal face.

Substitute Eq. (8) into Eq. (1), and it can be obtained.

$$\begin{cases} \sigma_x = \dfrac{12(y-h/2)}{h^3}\left[\int_0^x f(x)xdx - \dfrac{q}{2}(l+x)^2\right], \\ \tau_x = \dfrac{3}{2}\left(\dfrac{h^2-4y^2}{h^3}\right)\left[q(l+x) - \int_0^x f(x)dx\right]. \end{cases} \tag{9}$$

Huang et al., Hou, and Cai believed that the $f(x)$ distribution law of coal face should be satisfied as follows [30–32].

$$f(x) = \begin{cases} \dfrac{C}{\tan\varphi}\left(e^{(2\tan\varphi/mA)x} - 1\right), 0 < x \le x_0, \\ \gamma H - \dfrac{{x_0}^2}{x^2}(\gamma H - k\gamma H), x \ge x_0, \\ x_0 = \dfrac{mA}{2\tan\varphi}\ln\left(\dfrac{k\gamma H\tan\varphi}{C} + 1\right), \end{cases} \tag{10}$$

where C is the cohesive force of GWS, φ is the internal friction angle of coal and rock mass, k is the stress concentration factor, H is the burial depth of coal seam, m is the thickness of coal seam, A is the area of coal wall, and x_0 is the width of the plastic zone.

By substituting Eqs. (9) and (10) into Eq. (5), the stress distribution of GWS in CSBA under mining disturbance can be obtained:

$$\begin{cases} \sigma_\theta = \dfrac{12(y-h/2)}{h^3}\left[\int_0^x f(x)xdx - \dfrac{q}{2}(l+x)^2\right]\sin^2\theta - \dfrac{3}{2}\left(\dfrac{h^2-4y^2}{h^3}\right)\left[q(l+x) - \int_0^x f(x)dx\right]\sin 2\theta, \\ \tau_\theta = \dfrac{3}{2}\left(\dfrac{h^2-4y^2}{h^3}\right)\left[q(l+x) - \int_0^x f(x)dx\right]\cos 2\theta - \dfrac{6(y-h/2)}{h^3}\left[\int_0^x f(x)xdx - \dfrac{q}{2}(l+x)^2\right]\sin 2\theta. \end{cases} \tag{11}$$

3.3. Establishment of GWS Slip Criterion. The normal and tangential stresses of GWS in CSBA are the main influencing factors of triangular wedged rock block slip. Based on Coulomb's law of friction [33], the limit equilibrium condition of GWS should be satisfied as follows:

$$\tau_\theta = \sigma_\theta \tan\varphi + C. \tag{12}$$

Then, the ultimate shear strength of GWS is as follows:

$$F_\theta = \tau_\theta - \sigma_\theta \tan\varphi - C. \tag{13}$$

Due to the GWS in the CSBA having a spatial restriction effect on the triangular wedged rock block, the triangular wedged rock block will not move along the direction perpendicular to the coal-rock interface but only slip along the coal-rock interface direction. The slip criteria of GWS in the CSBA are as follows:

$$\begin{cases} F_\theta > 0, & \text{slip} \\ F_\theta \le 0, & \text{stabilization} \end{cases}. \tag{14}$$

Therefore, the factors affecting the slip of the GWS in the CSBA include the physical and mechanical parameters of the GWS, the coal seam stress concentration factor, the suspended length of the immediate roof, mining direction, and the mining situation of the coal face, as well as the angle and the height of the GWS in the CSBA. Excluding geological factors and mining technology factors, the important factors affecting the slip of the GWS in the CSBA are the angle and the height of the GWS in the CSBA. The height of the GWS in the CSBA can be expressed by the range and angle of the CSBA, which is also the main controlling factor affecting the slip of the GWS in the CSBA.

4. Numerical Simulation of GWS Slip in the CSBA

Based on the slip criterion of the GWS in the CSBA, it can be known that the key factors of the slip initiation are the range and angle of the CSBA. Numerical simulation is used to study the influence effect of main controlling factors to reveal the influence of these two factors on coal burst in CSBA.

4.1. Numerical Model and Numerical Simulation Scheme. The Extrusion module in FLAC3D can refine the occurrence structure of coal and rock in the CSBA and eliminate the modular scale effect of upper and lower strata in this area. Therefore, it is used to simulate the stress evolution characteristics of surrounding rock and the mechanical response characteristics of the GWS in the CSBA during the mining process.

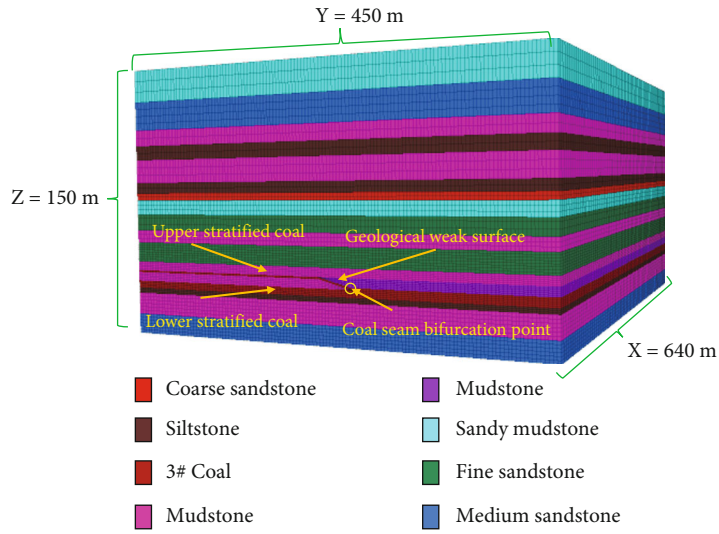

Figure 10: Numerical model.

Table 1: Mechanical parameters of coal and rock mass.

Lithology name	Density (kg/m^3)	Bulk modulus (GPa)	Shear modulus (GPa)	Cohesion (MPa)	Friction angle (°)	Tensile strength (MPa)
Sandy mudstone	2620	9.7	5.6	3.5	28	1.4
Medium sandstone	2740	12.1	6.8	3.7	33	2.3
Coarse sandstone	2700	10.1	5.2	3.2	31	2.2
Mudstone	1560	7.6	4.7	2.8	35	1.3
3# coal	1400	1.5	0.9	0.7	24	0.9
Fine sandstone	2810	14.3	7.6	4.0	36	2.5
Siltstone	2690	8.8	4.5	3.0	30	1.6

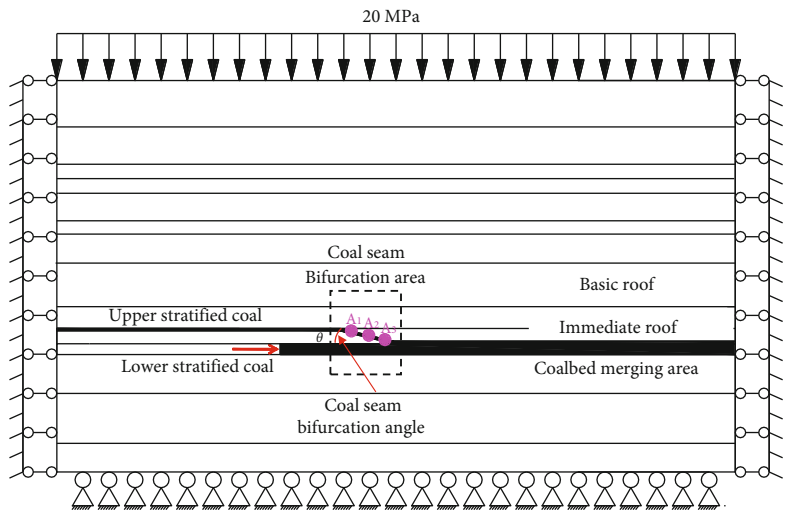

Figure 11: Layout of monitoring points in the numerical model.

As shown in Figure 10, based on geological and mining conditions of 1305CF, a numerical model with length, width, and height of 640 m, 450 m, and 150 m, respectively, was established. The model includes 839,500 grid units and 861,393 grid points to conform to the size effect [34]. The width of the coal face is 120 m, and the simulated advance recorded every 10 m of the coal face is 150 m. The height and width of roadway sections on both sides are 4 m and

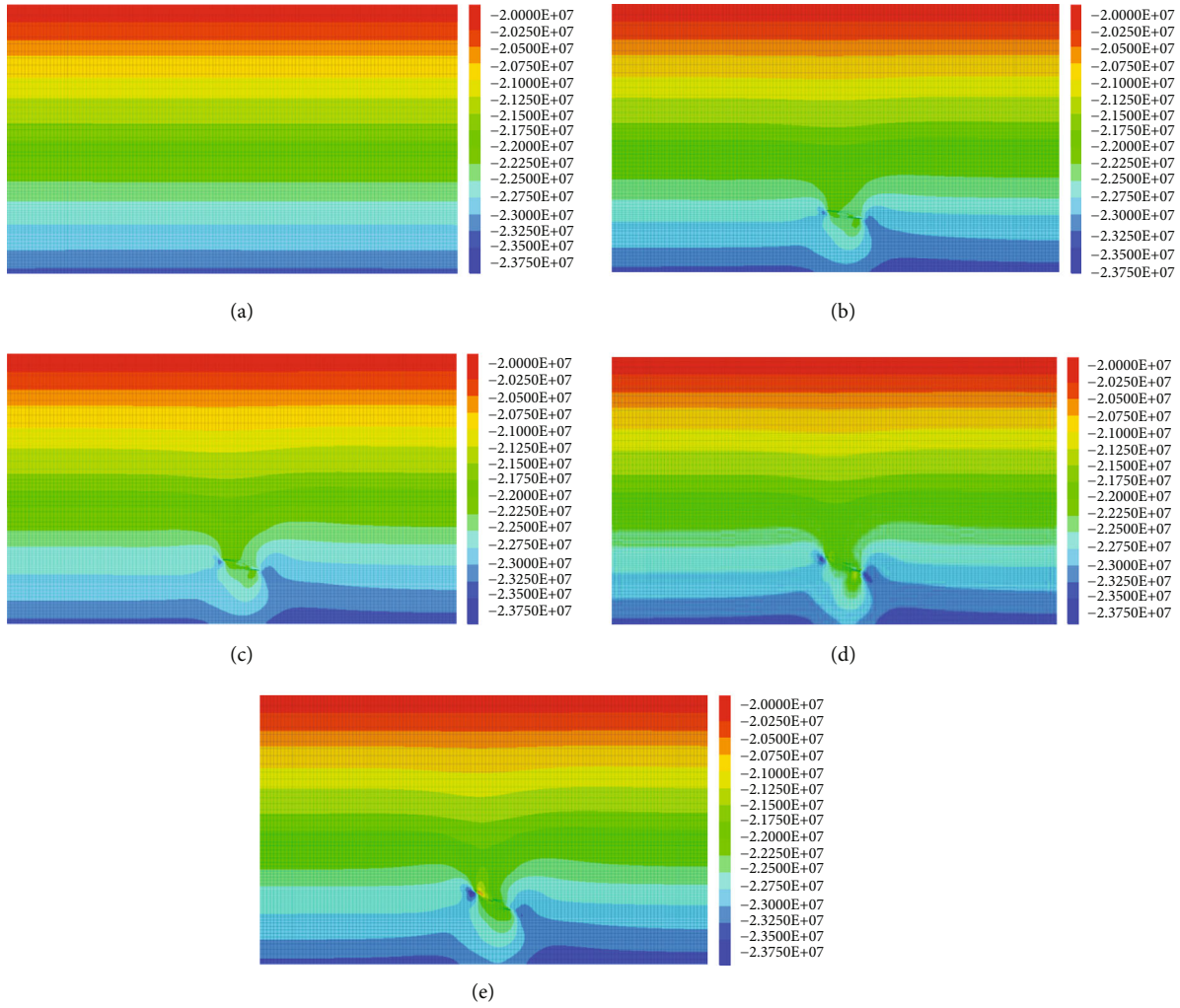

Figure 12: Cloud figure of primary rock stress based on the influence of the angle of CSBA: (a), (b), (c), and (d), respectively, represent 0, 10°, 15°, 20°, and 30°.

5 m, respectively. The boundary coal pillars with a width of 50 m were set around the stope, and the coal and rock follow the Coulomb-Mohr strength criterion. In the initial model, the thickness of the coalbed combined area was set to 5 m, while the thickness of the upper and lower coal seam in the CSBA was set to 1 m and 4 m, respectively. The angle of the CSBA was set to 15°, and the length of the CSBA was set to 20 m. Physical and mechanical parameters of 3# coal and rock strata in Zhaolou Coal Mine obtained from laboratory tests are shown in Table 1. Based on the initial model, the angle gradient of the CSBA was set as 10°, 15°, 20°, and 30°, and the gradient of the length of the CSBA was set as 10 m, 20 m, and 30 m.

20 MPa vertical stress was applied to the top of the model since the buried depth of the coal seam at 1305CF is about 950 m (see Figure 11). Based on the actual in situ stress test results of Zhaolou Coal Mine, the lateral pressure coefficient is 1.5. Therefore, 30 MPa horizontal stress was applied in the model's left and right directions, respectively. Three points A1, A2, and A3 with equal distance between two points on the GWS in the CSBA were selected to

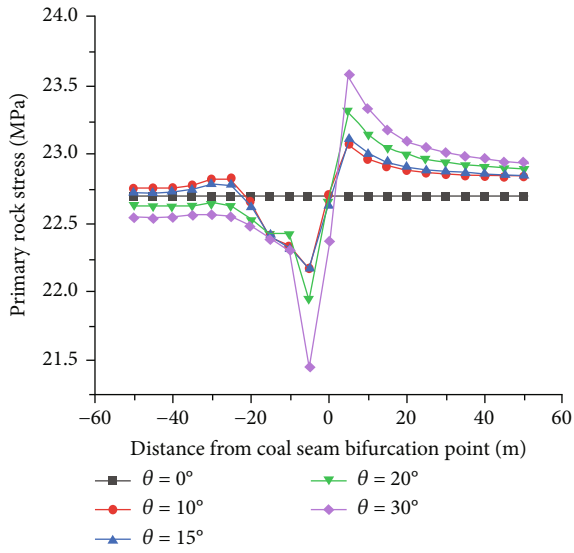

Figure 13: Primary rock stress distribution of mining coal seam based on the influence of the angle of CSBA.

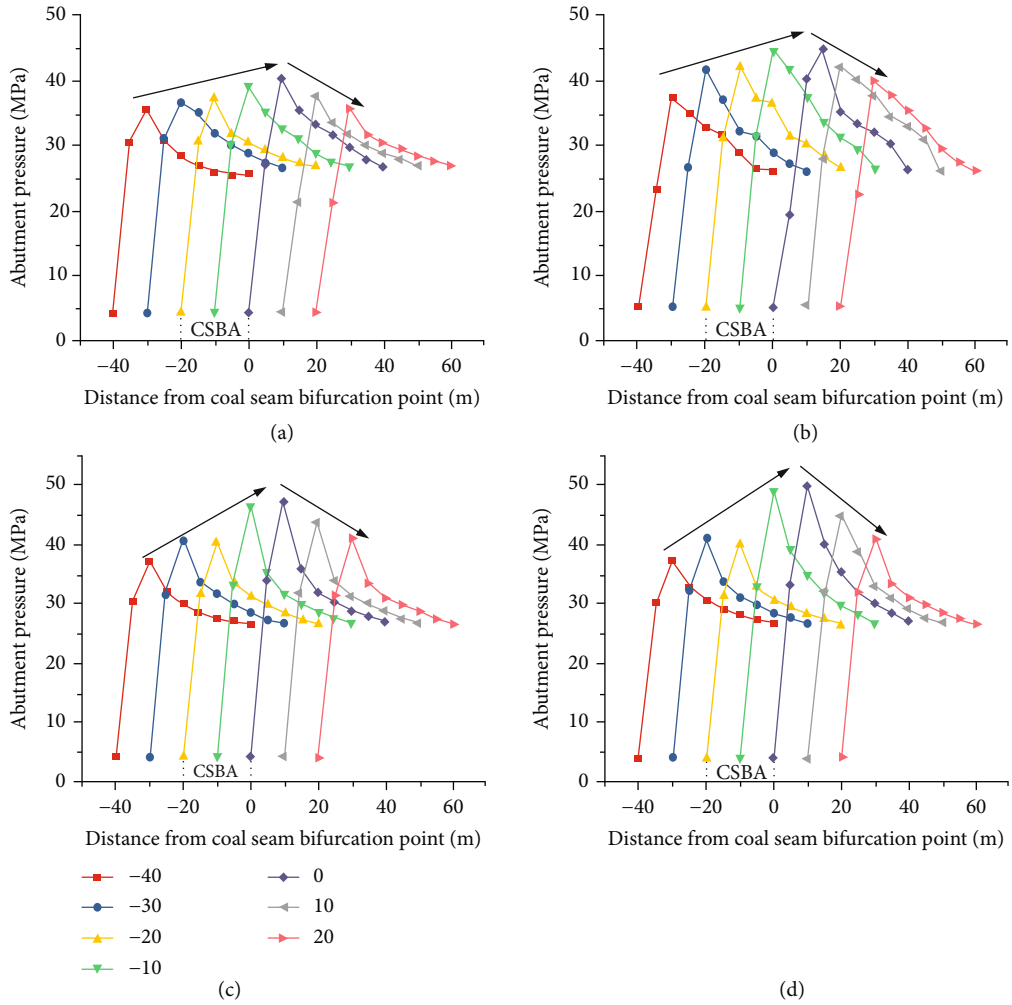

Figure 14: Distribution of abutment pressure of coal mass based on the influence of the angle of CSBA: (a), (b), (c), and (d), respectively, represent 10°, 15°, 20°, and 30°.

monitor normal and tangential stress changes. The triangular wedge rock block slides during the mining process can then be determined.

4.2. Effect Analysis of the Angle of CSBA. The fixed length of CSBA was set to 20 m, and the gradient of the angle of CSBA was set to 10°, 15°, 20°, and 30°. The stress distribution characteristics of surrounding rock and mechanical response characteristics of GWS at different bifurcation angles in the mining process were studied.

4.2.1. Distribution Characteristics of Primary Rock Stress. Figure 12 shows the distribution of primary rock stress at a different angle of CSBA. The larger the angle, the larger the stress anomaly area of primary rock stress. The primary rock stress near CSBA is concentrated at two tips, and the stress level of the upper and lower coal-rock stratum is lower than that of the coal-rock stratum at the same level, resulting in a large stress difference in the CSBA. Figure 13 shows distribution curves of primary rock stress of main coal seam (lower stratified coal seam) under different angles of CSBA. With the increase of angle of CSBA, the primary rock stress of the coal seam near the CSBA decreases first and then increases. The stress level of the lower stratified coal seam is lower due to the higher stress concentration in the turning point area of the upper bifurcation coal seam when approaching the CSBA. The coal seam becomes thicker, resulting in higher stress when gradually approaching the coalbed merging area. This indicates that the GWS causes the abnormal change of stress gradient in this area. It is easy to cause slip instability due to the excessive stress difference around the GWS in the CSBA when mining in this area. Therefore, with the angle increase of CSBA, the range of primary rock stress anomaly area also gradually becomes larger, the stress concentration degree of the coalbed merging area and the turning point area of the upper bifurcation coal seam gradually increase, and primary rock stress of the lower bifurcation coal mass in the CSBA gradually decreases, resulting in the larger stress gradient of the whole region.

4.2.2. Evolution Characteristics of Abutment Pressure of Coal Mass. Figure 14 shows the distribution curves of the abutment pressure of coal mass at different bifurcation angles. The results show that the angle of CSBA will affect the

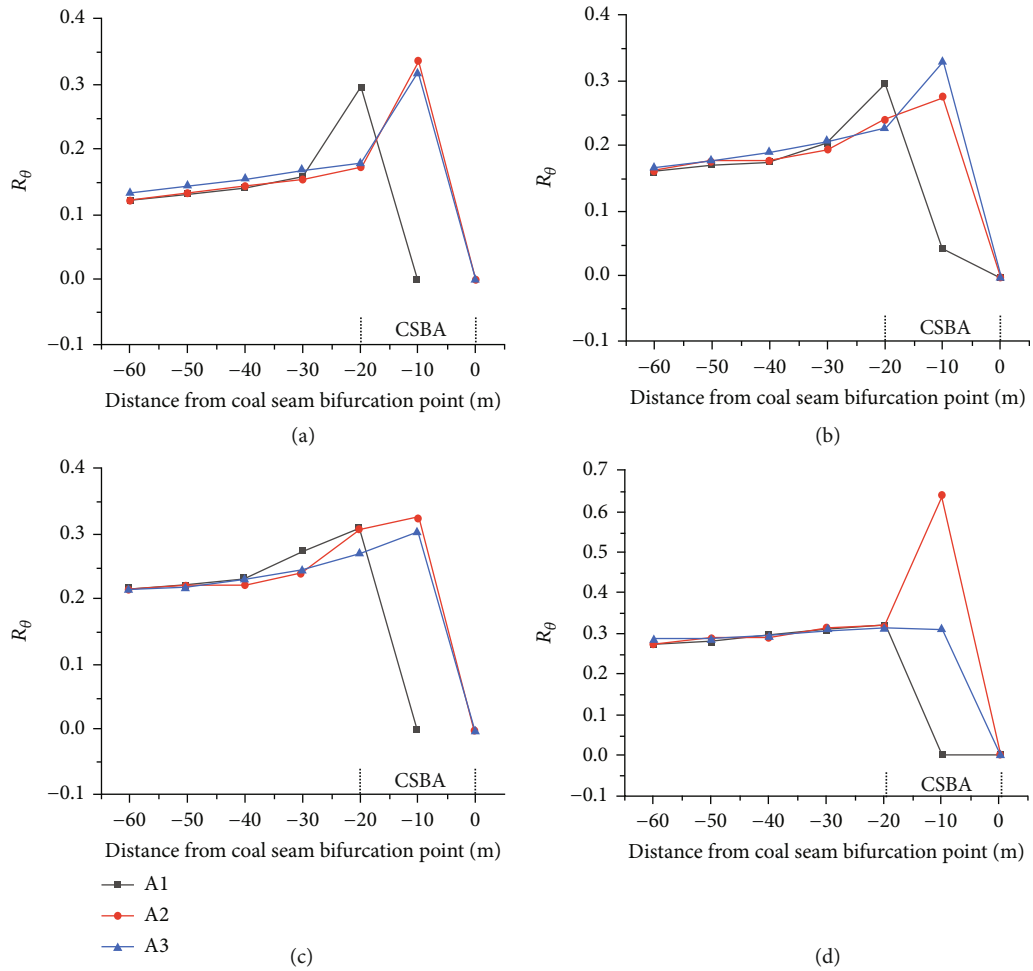

FIGURE 15: Evolution curve of the R_θ value based on the influence of the angle of CSBA during mining: (a), (b), (c), and (d), respectively, represent 10°, 15°, 20°, and 30°.

distribution of coal mass abutment pressure in the selected range of -40 m ~20 m from the coal face to the coal seam bifurcation line as the research area. The closer the coal face is to the coal seam bifurcation line, the higher the abutment pressure of the coal mass. The abutment pressure of coal mass reaches the highest when the coal face is mined within -10 m ~ 0 m from the coal seam bifurcation line. The abutment pressure peak value decreases gradually after the coal face is mined through the CSBA. Therefore, the peak value of coal mass abutment pressure gradually increases with the increase of the angle of CSBA, resulting in the gradually increased coal burst risk when the coal face crosses the CSBA. However, the increase of the angle of CSBA does not affect the peak point area of coal mass abutment pressure, which gradually reaches its peak within the range of 0 m ~10 m from the coalbed merge area.

In addition, the abutment pressure level does not rise significantly with increasing angle of CSBA when the coal face is mined at 20 m away from the coal seam bifurcation line. The abutment pressure peak value decreases slightly, especially when the angle of CSBA is 20° and 30°. This is because the stress concentration area of the coal face at this stage is distributed in the front coal mass and transferred to the GWS of the coal-rock interface with the increase of the angle of CSBA, forming a double stress concentration area. Therefore, the increase of the angle of CSBA will lead to the formation of a double stress concentration area near the GWS, further increasing the stress concentration coefficient of coal-rock mass.

4.2.3. Mechanical Response Characteristics of GWS. The activation of GWS depends on the numerical relationship between normal stress and tangential stress according to Eqs. (13) and (14). Therefore, the decrease of normal stress or the increase of tangential stress of the GWS may lead to slip, increasing the coal burst risk. The ratio of normal stress to tangential stress is defined as the tangential-normal stress ratio R_θ:

$$R_\theta = \frac{\tau_\theta}{\sigma_\theta}. \tag{15}$$

When the R_θ value increases gradually, the risk of GWS slip will increase. Therefore, it is necessary to record the evolution law of R_θ value on monitoring points A1, A2, and A3

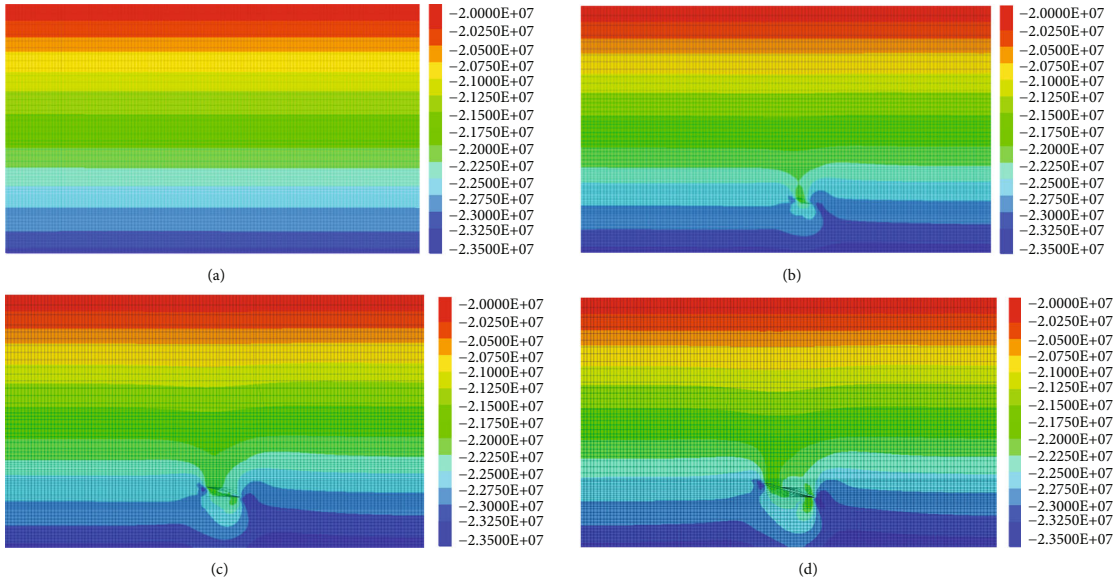

Figure 16: Cloud figure of primary rock stress based on the influence of the length of CSBA: (a), (b), (c), and (d), respectively, represent 0, 10 m, 20 m, and 30 m.

to analyze the slip instability of triangular wedged rock blocks.

As shown in Figure 15, the evolution law of R_θ value for each monitoring point on the GWS is the same. When the coal face approached the CSBA, the R_θ values of the three measuring points all showed an increasing-decreasing trend. At the high-order monitoring point A1, the R_θ value first reaches the peak value and then decreases when reaching the bifurcation area. When coal face reaches the CSBA, the R_θ value of high-order monitoring point A1 first reaches the peak value and then decreases. The R_θ value of the median-order monitoring point A2 and low-order monitoring point A3 reaches the peak value at 10 m away from the coalbed merging area and gradually decreases to 0 due to roof collapse. By comparing and analyzing each monitoring point peak value of the R_θ value, it is found that when the coal face is mined at 10 m away from the coalbed merging area, the peak value of the R_θ value increases with the increase of angle of CSBA, which is located in the middle of the GWS. The maximum R_θ value is 0.638 when the angle of CSBA is 30°, indicating that the thickness of triangular wedge rock is thicker, and the R_θ value is higher when the angle of CSBA is larger. The slip probability of the GWS reaches the maximum when the coal face advances to the middle section of the GWS. In the case of GWS slip, triangular wedged gangue with sufficient thickness will produce large extrusion pressure and dynamic load on the underlying coal mass, and this is easy to induce destructive coal burst accidents.

4.3. Effect Analysis of Length of CSBA. The fixed angle of CSBA was set to 15°, and the gradient of the length of CSBA was set to 10 m, 20 m, and 30 m. The stress distribution characteristics of surrounding rock and mechanical response characteristics of GWS at different bifurcation lengths in the mining process were studied.

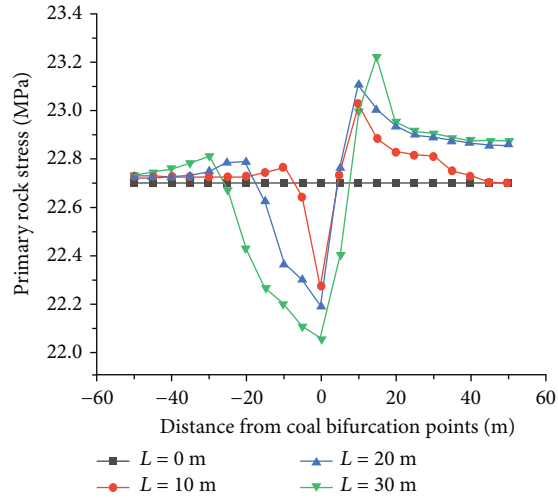

Figure 17: Primary rock stress distribution of mining coal seam based on the influence of the length of CSBA.

4.3.1. Distribution Characteristics of Primary Rock Stress. Figure 16 shows the distribution of primary rock stress at different lengths of CSBA. Figure 17 shows distribution curves of primary rock stress of main coal seam (lower stratified coal seam) under different angles of CSBA. The primary rock stress distribution under the length of CSBA is similar to that under the influence of the angle of CSBA. The primary rock stress near the CSBA decreases first and then increases with the CSBA length. When approaching the CSBA, the stress level of the lower stratified coal seam is lower due to the higher stress concentration in the turning point area of the upper bifurcation coal seam. However, the coal seam gradually becomes thicker when approaching the coalbed merging area, resulting in higher stress. With the increase of the length of the CSBA, the primary rock

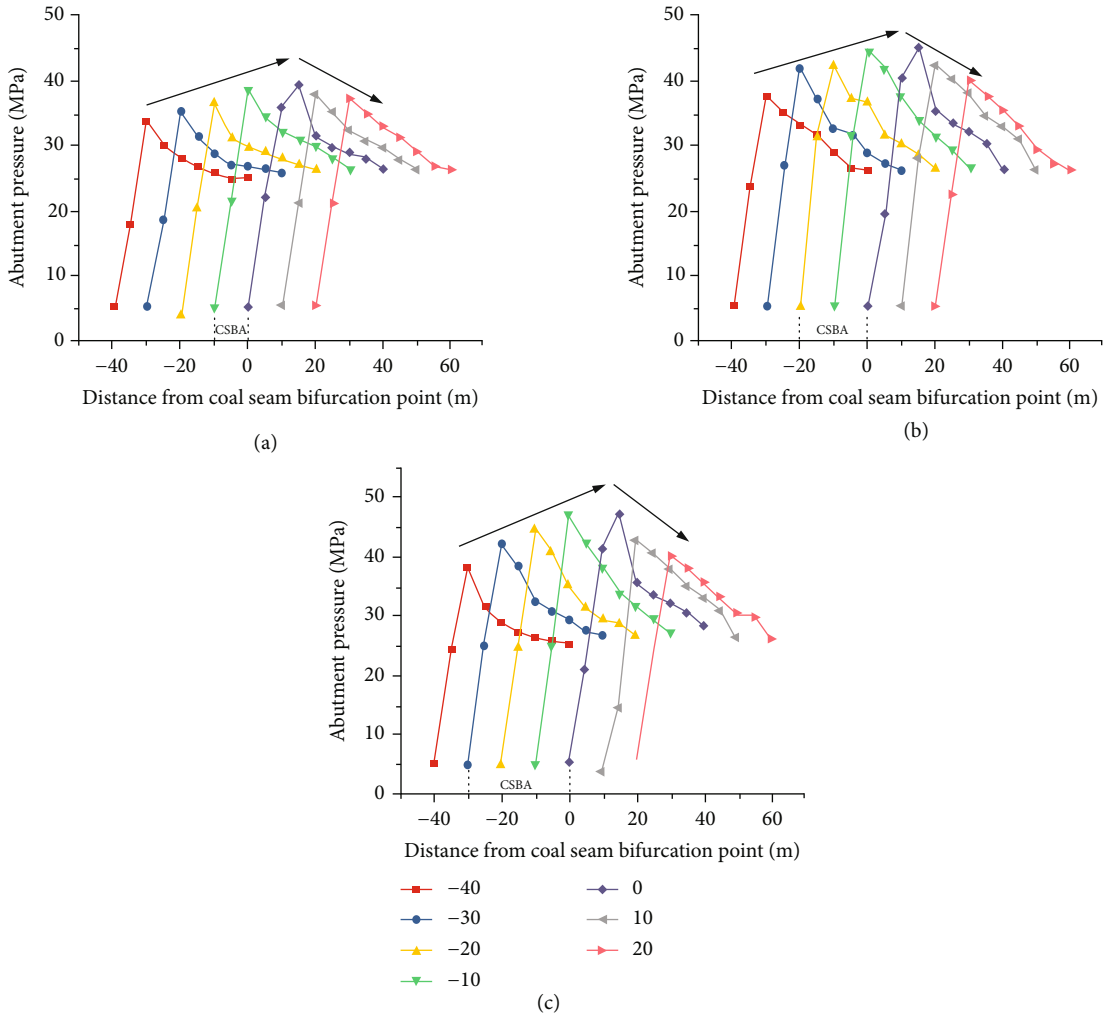

Figure 18: Distribution of abutment pressure of coal mass based on the influence of the length of CSBA: (a), (b), and (c), respectively, represent 10 m, 20 m, and 30 m.

stress near the CSBA is concentrated at the two tips of GWS, resulting in a large stress difference in the CSBA.

4.3.2. Evolution Characteristics of Abutment Pressure of Coal Mass. Figure 18 shows the distribution curves of abutment pressure of coal mass at different bifurcation lengths. The length of CSBA will affect the distribution of coal mass abutment pressure in the selected range of -40 m ~ 20 m from the coal face to the coal seam bifurcation line as the research area. When the coal face is mined within -10 m ~ 0 m from the coal seam bifurcation line, the abutment pressure of coal mass reaches the highest. The abutment pressure peak value decreases gradually after the coal face is mined through the CSBA. The peak value of abutment pressure of the same area increases gradually with the increase of the length of CSBA. Therefore, the peak value of abutment pressure of coal mass gradually increases with the increase of the length of CSBA, resulting in the coal burst risk increases when the coal face crosses the CSBA. However, the increase of CSBA length does not affect the peak point area of coal mass abutment pressure, which gradually reaches its peak within the range of 0 m ~10 m from the coalbed merge area.

4.3.3. Mechanical Response Characteristics of GWS. As shown in Figure 19, the evolution law of the three monitoring points on the GWS under the influence of the length of the CSBA is the same as that under the influence of the angle of the CSBA. The R_θ value of the three monitoring points all showed a trend of first increasing and then decreasing when the coal face approached the CSBA. The R_θ value of the three monitoring points reaches a peak simultaneously when the length of CSBA is 10 m. When the length of CSBA is 20 m, the R_θ value of high-order monitoring point A1 first reaches the peak value, followed by the R_θ value of the median-order monitoring point A2. The low monitoring-order point A3 reaches the peak value at 10 m away from the coalbed merging area. When the length of CSBA is 30 m, the R_θ value of high-order monitoring point A1 and median-order monitoring point A2 reaches their peak at 20 m away from the coalbed merging area, while the low-order monitoring point

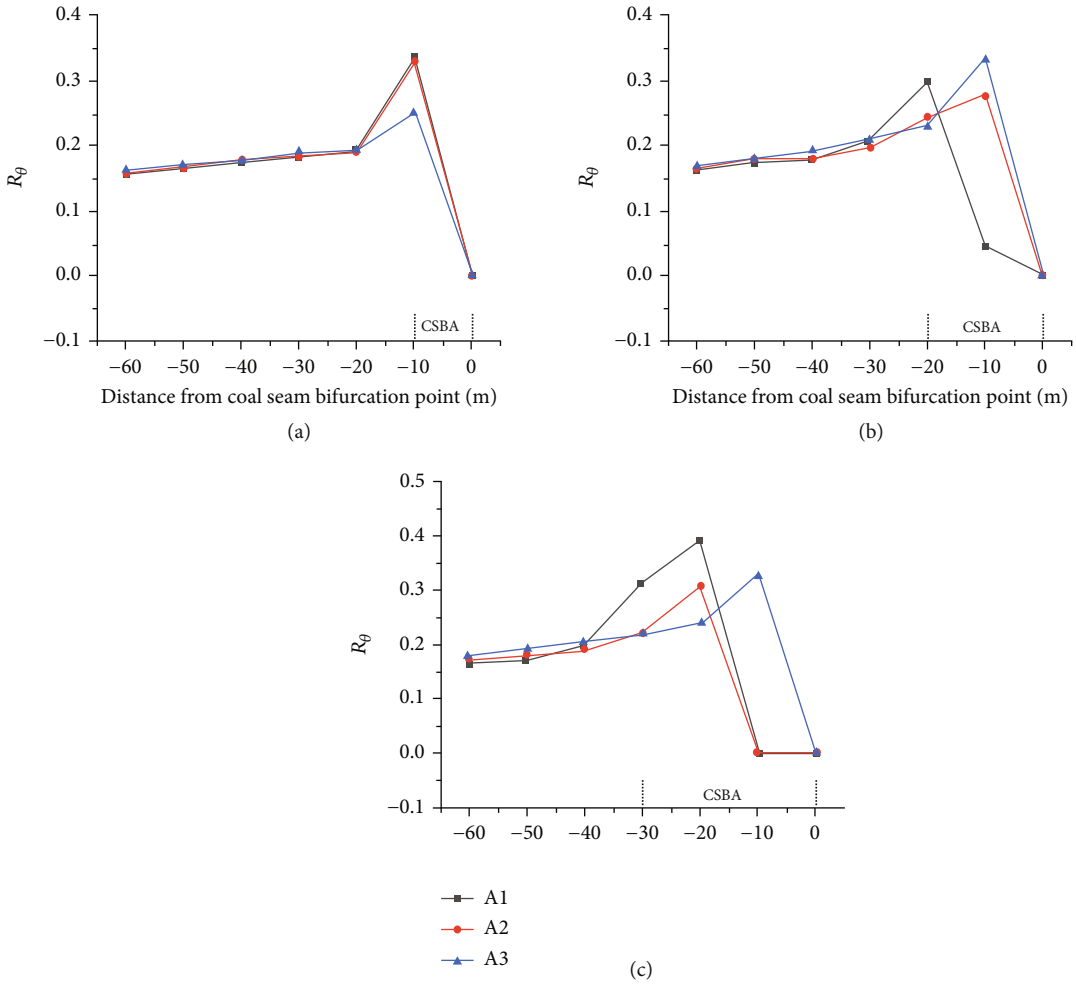

FIGURE 19: Evolution curve of the R_θ value based on influence of length of CSBA during mining: (a), (b), and (c), respectively, represent 10 m, 20 m and 30 m.

A3 reaches its peak 10 m away from the coalbed merging area. This indicates that the smaller the length of the CSBA, the easier it is for the GWS of the CSBA to induce the overall slip when the coal face is mined near the CSBA. The different level rock stratum on GWS will be disturbed gradually to induce stage slip of rock strata at different levels as the length of CSBA gradually increases, causing repeated extrusion disturbance to the coal mass of the coal face. The peak R_θ value increases with the increase of the length of CSBA, and the maximum R_θ value is 0.395 when the length of CSBA is 30 m. Moreover, it can also be found that the effect of the angle change of CSBA on the stress evolution of surrounding rock and the mechanical response of GWS is stronger than the length change of CSBA.

The long-distance CSBA is prone to periodic sliding of different layers of GWS regarding the intensity of coal burst accidents, causing repeated extrusion disturbance to the coal mass of coal face and making the coal mass easier to accumulate elastic energy induce destructive coal accident. It is easier to avoid coal burst accidents under the strengthening of support and pressure relief measures in the short-distance CSBA since both the gangue quality in the CSBA and the extrusion pressure on the coal mass are small.

5. Mechanism and Key Factors of Coal Burst Induced by GWS Slip in CSBA

The angle and the length (or range) of CSBA are the key factors to induce the GWS slip of CSBA according to the theoretical analysis and numerical simulation results. Based on the peak R_θ value index of monitoring points, it is found that the effect of the angle change of CSBA on the stress evolution of surrounding rock and the mechanical response of GWS is stronger than the length change of CSBA. The angle increase of CSBA will strengthen the integrity of triangular wedge rock mass sliding along the GWS, resulting in greater coal burst of the GWS slip instability. The length increase of CSBA will make the triangle wedged rock block slip along the GWS from the whole slip to the stage slip, presenting the stage disturbance to the coal mass of the coal face, which will increase the probability of coal burst.

The increase of angle (θ) and length (L) of CSBA will increase the abutment pressure of the coal seam and intensify the extrusion pressure on the coal mass of the coal face (see Figure 19). The slip of the GWS makes the gangue twist downward, forming extrusion (static load σ_s) and disturbance (dynamic load σ_{d1}) to the lower stratified coal mass. Meanwhile, the periodic breaking of the roof above the goaf also imposes dynamic load disturbance (dynamic load σ_{d2}) on the coal face. The superposition of dynamic and static load induces the coal burst accident in the CSBA under the coupling of multiple factors.

Figure 19 Schematic figure of induced coal burst factors in CSBA.

6. Conclusions

The mechanism and key factors of the coal burst accident were discussed by theoretical analysis and numerical simulations based on the coal burst accident of CSBA in 1305CF of Zhaolou Coal Mine. The main conclusions are as follows.

(a) Based on the mechanical analysis, the slip criterion of GWS in the CSBA was established. The analytic solution of stress distribution and slip criterion of GWS in the CSBA under the condition of original rock stress and mining disturbance were established by simplifying the overburden structure of CSBA, showing that the main controlling factors affecting the slip instability of GWS in CSBA were the angle and the range of the CSBA

(b) The FLAC3D numerical model was established to determine the effect of angle and length of CSBA on GWS slip. The larger the angle or length of CSBA, the larger the stress anomaly area of primary rock stress, and the higher the abutment pressure of coal mass, which will lead to the greater burst risk of the coal face passing through the CSBA. The angle increase of CSBA will strengthen the integrity of triangular wedge rock mass sliding along the geological weak plane, resulting in a more serious coal burst of the GWS. The triangle wedged rock block transforms from the whole slip to the stage slip along the GWS with CSBA length increase, indicating the stage disturbance to the coal mass of the coal face and the increased probability of coal burst

(c) Based on the theoretical analysis and numerical simulation results, the mechanism of coal burst induced by GWS slip in CSBA was determined. The slip of the GWS makes the gangue twist downward, forming extrusion and disturbance to the lower stratified coal mass. Meanwhile, the periodic breaking of the roof above the goaf also imposes dynamic load disturbance on the coal face. The superposition of dynamic and static load induces the coal burst accident in the CSBA under the coupling of multiple factors

Symbols

R: The internal force of the rock beam
q: Uniformly distributed load strength above rock strata
s: Length of rock stratum
σ_x: Normal stress in rock beam
τ_x: Tangential stress in rock beam
$M(x)$: The bending moment of the section at any point in the rock beam
$Q(x)$: The shear force of the section at any point in the rock beam
γ: Rock bulk density
h: Rock stratum thickness
θ: Angle of CSBA
L: Length of CSBA
σ_θ: Normal stress on GWS
τ_θ: Tangential stress on GWS
F_θ: Ultimate shear strength of GWS
R_θ: The ratio of tangential stress to normal stress on GWS
l: Suspended length of immediate roof
l_0: Distance from the coal face to coal seam bifurcation point
$f(x)$: Front abutment stress of coal face
C: Cohesive force of GWS
φ: Internal friction angle of coal and rock mass
k: Stress concentration factor
H: Burial depth of coal seam
m: The thickness of the coal seam
A: Area of coal wall
x_0: Width of plastic zone
σ_s: Static load on coal mass
σ_{d1}, σ_{d2}: Dynamic load on coal mass.

Data Availability

The relevant data used in this paper are available from the authors upon request.

Conflicts of Interest

The authors declare that they have no known personal relationships or competing economic interests that may affect the work reported in this work.

Acknowledgments

The authors gratefully acknowledge the financial support for this work provided by the National Natural Science Foundation of China (51974302, 42107177, 51874292).

References

[1] W. Cai, L. M. Dou, M. Zhang, W. Z. Cao, J. Q. Shi, and L. F. Feng, "A fuzzy comprehensive evaluation methodology for rock burst forecasting using microseismic monitoring," *Tunnelling and Underground Space Technology*, vol. 80, pp. 232–245, 2018.

[2] L. M. Dou, Z. L. Mu, Z. L. Li, A. Y. Cao, and S. Y. Gong, "Research progress of monitoring, forecasting, and prevention

of rockburst in underground coal mining in China," *International Journal of Coal Science and Technology*, vol. 1, no. 3, pp. 278–288, 2014.

[3] P. X. Li, X. T. Feng, G. L. Feng, Y. X. Xiao, and B. R. Chen, "Rockburst and microseismic characteristics around lithological interfaces under different excavation directions in deep tunnels," *Engineering Geology*, vol. 260, article 105209, 2019.

[4] B. Hebblewhite and J. Galvin, "A review of the geomechanics aspects of a double fatality coal burst at Austar Colliery in NSW, Australia in April 2014," *International Journal of Mining Science and Technology*, vol. 27, no. 1, pp. 3–7, 2017.

[5] C. Wei, C. Zhang, I. Canbulat, A. Y. Cao, and L. M. Dou, "Evaluation of current coal burst control techniques and development of a coal burst management framework," *Tunnelling and Underground Space Technology*, vol. 81, pp. 129–143, 2018.

[6] W. Cai, L. M. Dou, G. Y. Si et al., "A new seismic-based strain energy methodology for coal burst forecasting in underground coal mines," *International Journal of Rock Mechanics and Mining Sciences*, vol. 123, article 104086, 2019.

[7] A. Y. Cao, L. M. Dou, W. Cai, S. Y. Gong, S. Liu, and G. C. Jing, "Case study of seismic hazard assessment in underground coal mining using passive tomography," *International Journal of Rock Mechanics and Mining Sciences*, vol. 78, pp. 1–9, 2015.

[8] S. Y. Gong, J. Li, F. Ju, L. M. Dou, J. He, and X. Y. Tian, "Passive seismic tomography for rockburst risk identification based on adaptive-grid method," *Tunnelling and Underground Space Technology*, vol. 86, pp. 198–208, 2019.

[9] Z. L. Mu, G. J. Liu, J. Yang et al., "Theoretical and numerical investigations of floor dynamic rupture: a case study in Zhaolou coal mine, China," *Safety Science*, vol. 114, pp. 1–11, 2019.

[10] J. He, L. M. Dou, S. Y. Gong, J. Li, and Z. Ma, "Rock burst assessment and prediction by dynamic and static stress analysis based on micro-seismic monitoring," *International Journal of Rock Mechanics and Mining Sciences*, vol. 93, pp. 46–53, 2017.

[11] Z. L. Mu, J. Yang, J. H. Jiao et al., "Application of strong pressure relief technology in deep isolated working face," *Coal Science and Technology Magazine*, vol. 42, no. 2, pp. 10–23, 2021.

[12] L. M. Dou, A. L. Lu, J. R. Cao, J. Z. Bai, J. J. Liu, and H. J. Ma, "Study on stress-energy evolution law of irregular coal pillar in double coal seam and anti-flushing technology," *Coal Science and Technology Magazine*, vol. 42, no. 2, pp. 1–9, 2021.

[13] Y. Y. Lu, C. P. Song, Y. Z. Jia et al., "Analysis and numerical simulation of hydrofracture crack propagation in coal-rock bed," *CMES-Computer Modeling in Engineering & Sciences*, vol. 105, no. 1, pp. 69–86, 2015.

[14] B. B. Chen, C. Y. Liu, and B. Wang, "A case study of the periodic fracture control of a thick-hard roof based on deep-hole pre-splitting blasting," *Energy Exploration & Exploitation*, vol. 40, no. 1, pp. 279–301, 2021.

[15] M. Zhang, L. M. Dou, H. Konietzky, Z. Y. Song, and S. Huang, "Cyclic fatigue characteristics of strong burst-prone coal: experimental insights from energy dissipation, hysteresis and micro-seismicity," *International Journal of Fatigue*, vol. 133, article 105429, 2020.

[16] L. M. Dou, J. He, A. Y. Cao, S. Y. Gong, and W. Cai, "Rock burst prevention methods based on theory of dynamic and static combined load induced in coal mine," *Journal of China Coal Society*, vol. 40, no. 7, pp. 1469–1476, 2015.

[17] L. M. Dou, K. Y. Zhou, S. K. Song et al., "Research progress of monitoring, forecasting, and prevention of rockburst in underground coal mining," *Journal of Engineering Geology*, vol. 29, no. 4, pp. 917–932, 2021.

[18] C. B. Wang, A. Y. Cao, C. G. Zhang, and I. Canbulat, "A new method to assess coal burst risks using dynamic and static loading analysis," *Rock Mechanics and Rock Engineering*, vol. 53, no. 3, pp. 1113–1128, 2019.

[19] Y. Xue, Z. Z. Cao, and Z. H. Li, "Destabilization mechanism and energy evolution of coal pillar in rockburst disaster," *Arabian Journal of Geosciences*, vol. 13, no. 13, pp. 1–13, 2020.

[20] C. H. Song, C. P. Lu, X. F. Zhang et al., "Moment tensor inversion and stress evolution of coal pillar failure mechanism," *Rock Mechanics and Rock Engineering*, vol. 55, no. 4, pp. 2371–2383, 2022.

[21] G. F. Wang, S. Y. Gong, L. M. Dou, H. Wang, W. Cai, and A. Y. Cao, "Rockburst characteristics in syncline regions and microseismic precursors based on energy density clouds," *Tunnelling and Underground Space Technology*, vol. 81, pp. 83–93, 2018.

[22] J. He, L. M. Dou, Z. L. Mu, A. Y. Cao, and S. Y. Gong, "Numerical simulation study on hard-thick roof inducing rock burst in coal mine," *Journal of Central South University*, vol. 23, no. 9, pp. 2314–2320, 2016.

[23] W. Cai, L. M. Dou, G. Y. Si, and Y. W. Hu, "Fault-induced coal burst mechanism under mining-induced static and dynamic stresses," *Engineering*, vol. 7, no. 5, pp. 687–700, 2021.

[24] A. Sainoki and H. S. Mitri, "Effect of slip-weakening distance on selected seismic source parameters of mining-induced fault-slip," *International Journal of Rock Mechanics and Mining Sciences*, vol. 73, pp. 115–122, 2015.

[25] H. Z. Xu, "Study on the splitting mechanism of coal seam no. 3 of Shanxi Formation in Southwest Shandong Province," *Journal of Shandong University of Science and Technology*, vol. 22, no. 2, pp. 37–40, 2003.

[26] H. Wang, *Research on the Prevention and Mechanism of Coal Burst Induced by Geological Weak-Plane Tensile-Slip Activities during Mining*, China University of mining and technology, Beijing, 2018.

[27] P. Kong, L. S. Jiang, J. M. Shu, and L. Wang, "Mining stress distribution and fault-slip behavior: a case study of fault-influenced longwall coal mining," *Energies*, vol. 12, no. 13, article 2494, 2019.

[28] C. T. Holland, "Cause and occurrence of coal mine bumps trans," *SME-AIME*, vol. 211, no. 13, pp. 994–1004, 2058.

[29] M. Alber, R. Fritschen, M. Bischoff, and T. Meier, "Rock mechanical investigations of seismic events in a deep longwall coal mine," *Journal of Rock Mechanics and Mining Sciences*, vol. 46, no. 2, pp. 408–420, 2009.

[30] Q. X. Huang, M. G. Qian, and P. W. Shi, "Structural analysis of main roof stability during periodic weighting in longwall face," *Journal of China Coal Society*, vol. 24, no. 6, pp. 581–585, 1999.

[31] C. J. Hou, *Ground Control Roadways*, China University of mining and Technology Press, Xuzhou, 2013.

[32] M. F. Cai, *Rock Mechanics and Engineering*, Science Press, Beijing, 2013.

[33] M. K. Hubbert and W. W. Rubey, "Role of fluid pressure in mechanics of overthrust faulting," *Geological Society of America Bulletin*, vol. 70, no. 2, pp. 115–166, 1959.

[34] Z. Z. Liang, Y. B. Zhang, S. B. Tang, L. C. Li, and C. A. Tang, "Size effect of rock messes and associated representative element properties," *Chinese Journal of Rock Mechanics and Engineering*, vol. 32, no. 6, pp. 1157–1166, 2013.